

How is experience transformed into memory?

Andrew C. Heusser, Paxton C. Fitzpatrick, and Jeremy R. Manning

Department of Psychological and Brain Sciences

Dartmouth College, Hanover, NH 03755, USA

Corresponding author: jeremy.r.manning@dartmouth.edu

August 28, 2018

Abstract

How our experiences unfold over time define unique *trajectories* through the relevant representational spaces. Within this geometric framework, one can compare the shape of the trajectory formed by an experience to that defined by our later remembering of that experience. We propose a framework for mapping naturalistic experiences onto geometric spaces that characterize how they unfold over time. New insights emerge when we apply this approach to a naturalistic memory experiment which had participants view and recount a video. We found that the shapes of the trajectories formed by participants' recounts were all highly similar to that of the original video, but participants differed in the level of detail they remembered. We also identified a network of brain structures that are sensitive to the "shapes" of our ongoing experiences, and an overlapping network that is sensitive to how we will later remember those experiences.

Introduction

What does it mean to *remember* something? In traditional episodic memory experiments (e.g., list-learning or trial-based experiments; Murdock, 1962; Kahana, 1996), remembering is often cast as a discrete and binary operation: each studied item may be separated from the rest of one's experiences, and that item may be labeled as having been recalled versus forgotten. More nuanced studies might incorporate self-reported confidence measures as a proxy for memory strength, or ask participants to discriminate between "recollecting" the (contextual) details of an experience or having a general feeling of "familiarity" (Yonelinas, 2002). However, characterizing and evaluating memory in more realistic contexts (e.g., recounting a recent experience to a friend) is fundamentally different in at least three ways (also see Kriat and Goldsmith, 1994, for a review). First, real world recall is continuous, rather than discrete. Unlike in trial-based experiments, removing a (naturalistic) event from the context in which it occurs can substantially change its meaning. Second, the specific words used to describe an experience have little bearing on whether the experience should be considered to have been "remembered." Asking whether the rememberer has precisely reproduced a specific set of words to describe a given experience is nearly orthogonal to whether they were actually able to remember it. In classic (e.g., list-learning) memory studies, precise recall is often a primary metric of assessing the quality of participants' memories. Third, one might remember the gist or essence of an experience but forget (or neglect to recount) particular

details. Capturing the *gist* of what happened is typically the main “point” of recounting a memory to a listener whereas, depending on the circumstances, accurate recall of any specific detail may be irrelevant. There is no analog of the “*gist*” of an experience in most traditional memory experiments; rather we tend to assess participants’ abilities to recover specific details (e.g., the precise stimuli they encountered earlier in the experiment).

How might one go about formally characterizing the “*gist*” of an experience? Any given moment of an experience derives meaning from surrounding moments, as well as from longer-range temporal associations (e.g., Lerner et al., 2011). Therefore the timecourse of how an event unfolds is fundamental to its overall meaning. Further, this hierarchy formed by our subjective experiences at different timescales defines a *context* for each new moment (e.g., Howard and Kahana, 2002; Howard et al., 2014), and plays an important role in how we interpret that moment and remember it later (for review see Manning et al., 2015). Our memory systems can then leverage these associations to form predictions that help guide our behaviors (Ranganath and Ritchey, 2012). For example, as we navigate the world, the features of our subjective experiences tend to change gradually (e.g. the room or situation we are in is strongly temporally autocorrelated), allowing us to form stable estimates of our current situation and behave accordingly (Zacks et al., 2007; Zwaan and Radvansky, 1998). Although our experiences typically change gradually, they also occasionally change suddenly (e.g., when we walk through a doorway; Radvansky and Zacks, 2017). Prior research suggests that these sharp transitions (termed *event boundaries*) during an experience help to discretize our experiences into *events* (Radvansky and Zacks, 2017; Brunec et al., 2018; Heusser et al., 2018; Clewett and Davachi, 2017; Ezzyat and Davachi, 2011; DuBrow and Davachi, 2013). The interplay between the stable (within event) and transient (across event) temporal dynamics of an experience also provides a potential framework for transforming experiences into compressed memories. For example, prior work has shown that event boundaries can influence how we learn sequences of items (Heusser et al., 2018; DuBrow and Davachi, 2013), navigate (Brunec et al., 2018), and remember and understand narratives (Zwaan and Radvansky, 1998; Ezzyat and Davachi, 2011).

Here we sought to examine how the temporal dynamics of a “naturalistic” experience were reflected in participants’ later memories of that experience. We analyzed an open dataset which comprised behavioral and functional Magnetic Resonance Imaging (fMRI) data collected as participants viewed and then verbally recalled an episode of the BBC television series *Sherlock* (Chen et al., 2017). We developed a computational framework for characterizing the temporal dynamics of the moment-by-moment content of the episode (and of participants’ verbal recalls). Specifically, we use topic modeling (Blei et al., 2003) to characterize the thematic conceptual (semantic) content present in each moment of the episode and recalls, and we use Hidden Markov Models (Rabiner, 1989; Baldassano et al., 2017) to discretize the evolving semantic content into events. In this way, we cast naturalistic experiences (and recalls of those experiences) as *topic trajectories* that describe how the experiences evolve over time. In other words, the episode’s topic trajectory is a formalization of its *gist*. Under this framework, successful remembering entails verbally “traversing” the topic trajectory of the original episode, thereby reproducing the *gist* of the original episode. In addition, comparing the shapes of the topic trajectories of the original episode and of participants’ retellings of the episode reveals which aspects of the episode were preserved (or lost) in the translation into memory. We also identified a network of brain structures whose responses (as participants watched the episode) reflected the *gist* of the episode, and a second network whose responses reflected how participants would later recount the episode.

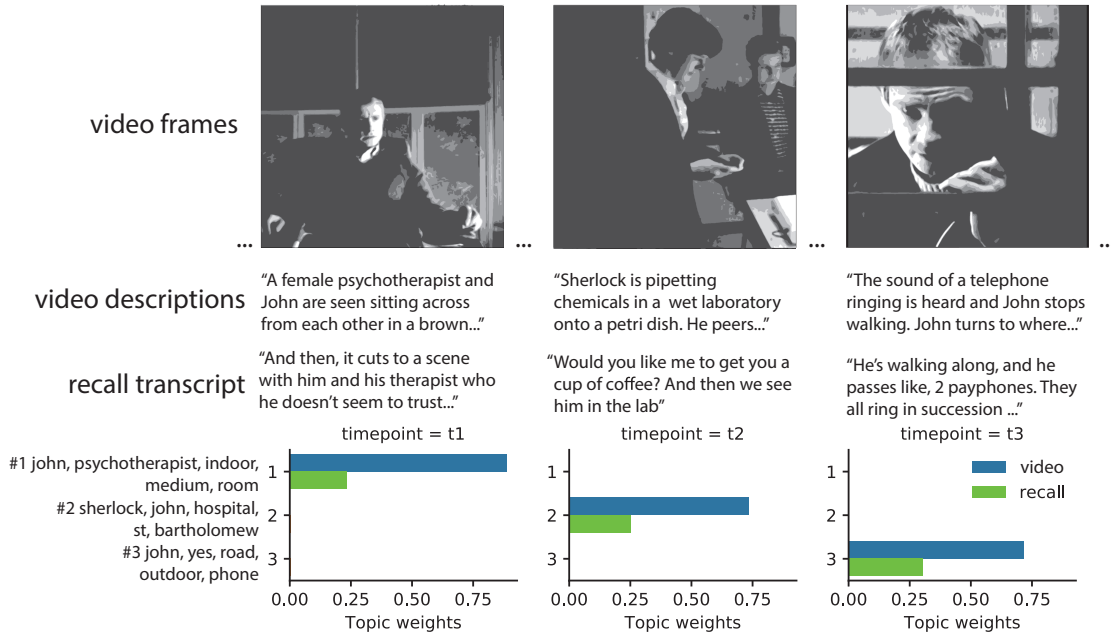


Figure 1: Schematic of the analysis approach. For each scene in the video, text descriptions were generated by hand. Three exemplary time points are displayed here. Below the video descriptions are text samples from an example participant’s verbal recall transcript. We fit a topic model to the moment-by-moment video text descriptions and transformed participants’ verbal recall transcripts using this same model. The bar charts display the resulting topic model weights for the video (in blue) and recall (in green) for three example topic dimensions.

Results

Modeling the naturalistic stimulus and verbal recall

We fit a topic model (Blei et al., 2003) to hand-annotated text descriptions of scenes from the video. The text descriptions contained details of the scene such as the characters present, location, and a short summary of the scene (see Fig. 1 for example text). As depicted in Fig. 2A, the topic vectors are sparse and change slowly over time. Furthermore, there are clear transitions from one topic “state” to the next, possibly indexing scene transitions in the stimulus. To get a better handle on this temporal structure, we computed a timepoints (1976) by timepoints (1976) correlation matrix of the video model (Fig. 2C). This correlation matrix reveals that the model has a strong, block-diagonal structure with very low off-diagonal correlation values, suggesting the representations of each block are unique and highly discriminable. We found that the “narrative details” (a few sentences summarizing the dialogue and specific happenings of the scene) of the video were the most important feature driving this model structure (see Supp. Fig. 3A).

After watching the video, participants verbally recalled (in order) as much of the episode as they could. We used the same topic model (fit with the text descriptions of the video) to

transform participants' verbal recall transcripts. An example participant's (#13) recall model is plotted in Fig. 2B. Notably, participant #13's recall model appears visually similar to the video model. Similar to the video model analysis (Supp. Fig. 3A), we found that the "narrative details" feature was most important for driving the video/recall relationship (Supp. Fig. 3B). Like the video model, topic vectors were sparse and changed gradually. Then, we investigated the temporal structure of the recall matrices. From each participant's recall model, we computed a sentences (68 to 294) by sentences (68 to 294) correlation matrix (Fig. 2D). Like the video model, each participant's recall correlation matrix exhibited a strong block-diagonal structure (Supp. Fig. 1). Notably, this suggests that participants recounted the video in discriminable segments, likely related to the recall of specific events from the video.

Segmenting the video and recall models into "events"

As described above, a striking feature of both the video and recall correlation matrices is a strong, block structure along the diagonal of the matrices (see Fig. 2C,D). We hypothesized that this structure might arise from transient stability in the "theme" of both the video and of participants' memory for the video. We hypothesized that specific events described by a participant could be "matched" to specific video events by computing the similarity (i.e., correlation) between their topic vectors. In other words, the video event that is most thematically similar to a particular recall event is the event that the participant is most likely describing. To test this idea, we segmented the video and recall models in k events (i.e., states) using a hidden Markov model (Baldassano et al., 2017). Our algorithm determined 34 events for the video model and a range of values (range: 8-27; mean: 15.41; SD: 5.6) for the recall models (see Methods for details on choosing an optimal k value). The events discovered for the video model and a representative participant's recall model are highlighted as yellow rectangles outlining blocks along the diagonal of the correlation matrices (Fig. 2C,D).

Next, we created a video "event model" by averaging together neighboring topic vectors that were classified to be in the same event, resulting in an events (34) by topics (100) matrix (Fig. 2E). We performed the same procedure for the recall matrices (Fig. 2F). Then, we computed the correlation between video and recall event models, resulting in a video events (34) by recall events (8-27, depending on the participant) correlation matrix (Fig 2G for example, Supp. Fig 2 for all participants). These matrices represent the similarity (correlation) between each video event and each recall event (for each participant). To determine which video event a particular recall event was most likely describing, we found the index of the video event with the highest correlation to the recall event (i.e., the argmax). This is depicted in Fig. 2G as the cells highlighted with a yellow border. Notably, our algorithm suggests that the example participant recalled most of the video events and did so in order.

Then, we computed a group-averaged recall event model and video-recall event correlation matrix. For each participant (and each recall event), we sorted the recall event vectors (across all participants) according to the video event with the highest correlation. We then averaged the recall event vectors within each group. This yielded an average recall event vector for all but one (of 34) video events, since no participant remembered one of the events according to our model. Lastly, we computed an average recall event (34) by video event (34) correlation matrix, and highlighted the cell with the highest correlation value with a yellow border (Fig. 2H). Notably, this matrix displayed high correlation values along the diagonal and low correlations in the off-diagonal cells. This suggests that on average, participants were able to recapitulate the events in the episode in a

specific, sequential and highly discriminable way.

The trajectory of a naturalistic experience is preserved in recall

Classic approaches to studying free recall in episodic memory (such as overall accuracy and serial position curve) focus on the quantity of information recalled (Murdock, 1962). More recent metrics (such as lag-CRP, semantic and temporal clustering) go further to describe list-level memory organization (Kahana, 1996; Polyn et al., 2009). However, these approaches cannot (and were not designed to) capture the rich temporal dynamics inherent in naturalistic stimuli and associated recall of those experiences. In the next set of analyses, we test the hypothesis that successful recall of a naturalistic stimulus entails recovering the trajectory of a stimulus.

To visualize the relationship between the video and recall event models, we embedded them into a 2D space using the UMAP dimensionality reduction algorithm (McInnes and Healy, 2018), where the points represent video/recall events and the distance between them represents their similarity/distance in “topic space” (Fig. 3A). We observed that visually, it appears that the two models have a very similar temporal evolution and geometric structure. To further quantify this correspondence and to characterize how participants navigated through the space during recall, we analyzed the angle between successive recall events. We created a grid of evenly spaced points (.25 units) in the 2D “topic space.” For each point on the grid, we drew a circle (radius=.5) around the point and grouped together all recall transitions that intersected the circle (across participants). To visualize the average angle, we converted each transition angle to a unit vector and then averaged the vectors together. To assess consistency in the direction of the recall transition across participants, we performed a Rayleigh test ($p < .001$, corrected at $p < .05$ using the permutation procedure described in Methods). Notably, the video events fell within the path formed by the recall events. Thus, participants’ recalls followed the same path as the video model (Fig. 3B), suggesting the shape of the stimulus was preserved despite idiosyncratic differences between participants in their recalls.

Brain regions that mirror the correlational structure of naturalistic stimuli and memories

Previous work suggests that the brain may represent our experiences as “events” with different time scales in a nested hierarchy (Lerner et al., 2011; Chen et al., 2017; Baldassano et al., 2017). In this next analysis we asked: what brain regions mirror the event-like correlational structure of our topic-based video model during viewing? We used a searchlight procedure (see Methods for details) to identify regions whose timepoint-by-timepoint correlational structure matched the correlational structure of our model. This analysis revealed a network of regions including bilateral frontal and cingulate cortex (Fig. 4), suggesting that these regions may play a role in maintaining information relevant to the narrative trajectory of the video.

While each participant remembered roughly the same sequence of events, there were subtle idiosyncrasies in the way each individual described the events. For example, the event-by-event similarity structure (i.e., the off-diagonal values of the recall correlation matrices) differed across individuals (Supp. Fig. 1). We hypothesized that idiosyncrasies in the recall dynamics across participants might be related to the temporal structure of brain networks representing the events during video viewing. In this analysis, we identified brain areas whose responses at the time

of viewing exhibited the same (segmented) idiosyncratic dynamics that later appeared in that participants' recalls. Using a procedure similar to the approach above (see Methods for details), we searched for regions whose correlational structure during viewing was related to the idiosyncratic structure of the participant's recall model. The resulting map suggests that the correlational structure of a network of brain regions including the ventromedial prefrontal cortex, anterior cingulate, and right medial temporal lobe mirror the idiosyncratic structure of participants' recalls (Fig. 4).

Memorability by event and topics

A notable advantage of representing naturalistic stimuli and memory using this approach is that the event models can be mapped back to the language used to fit the model(s). This allows for analysis (and visualization) of the language used when participants recounted their experiences. In this next analysis, we 1) quantified the memorability of each video event and 2) used memorability to plot the "top" words for the most and least memorable scenes.

To measure video event memorability, we computed the correlation between each video event and the closest recall event and then averaged those values within participants (Fig. 5A). We used event memorability to create a weighted average over all video event vectors, where video events with better memory were weighted more heavily. Then, we extracted the top 200 words and created "wordles" representing the most memorable themes in the video. The results reveal that scenes containing "Sherlock" and "John" were highly memorable, as were scenes containing words such as "medium", "street" and "baker" (Fig. 5B). To find words related to the least memorable scenes, we inverted the memorability weights and again extracted the top 200 words. Scenes containing "Mike" and "Molly" were least remembered, and also words like "conference", "hospital" and "psychotherapist" (Fig. 5B).

Then, we took a closer look at the themes contained in the top/bottom 3 events, using the memorability weights to select the top/bottom events. We performed the same analysis as described above, but separately for the video and average recall event vectors representing each of the top/bottom 3 remembered events. In Figure 5C, the trajectory represents a low-dimensional embedding of the video model and the large colored dots represent the video events. The smaller colored dots represent the distribution of individual recall events across all participants, colored by the closest video event. We plotted wordles for the top 3 (circled in green) and bottom 3 (red) most/least remembered events, where the video is represented in the left half of the circle and the average recall is represented in the right half of the circle. Visual inspection reveals that the words contained in the memorability weighted wordles (Fig. 5B) overlap with the individual top/bottom event wordles (Fig. 5C). These analyses shed light on the contents of naturalistic stimuli and accompanying memories, and highlight the flexibility in transforming between human and machine readable representations of the data afforded by our modeling approach.

Additional measures of naturalistic recall

Representing the video and verbal recall as events in "topic space" also affords us the ability to characterize the quality of recall in a more fine-grained and nuanced way than was previously possible. We quantified the distance between each video event and its matching recall event ("precision"), the the distance between a video event and all non-matching recall events ("distinctiveness") and the temporal order of the recall events ("order"). All three of these metrics were

correlated to hand-annotated memory performance across participants ($p < .05$, see Supplemental Materials Section 1 for details).

Just like in a traditional free recall list-learning experiment where participants view a list of words and then verbally recall them, our video-recall matching analysis approach affords us the ability to analyze memory in the same way. We considered 6 classic list-learning analyses: overall accuracy, probability of first recall (Hogan, 1975; Howard and Kahana, 1999; Laming, 1999), lag-conditional response probability (Kahana, 1996; Howard and Kahana, 1999), serial position curve (Murdock, 1962), temporal clustering, and semantic clustering (Howard and Kahana, 2002; Polyn et al., 2009). Extending these classic list-learning analyses to naturalistic stimuli allows to directly compare trial- and naturalistic-based recall studies (see Supplemental Materials Section 2 for details).

Discussion

Studying human memory is commonly distilled down to a process of matching specific moments of a past experience with specific mnemonic outcomes. In traditional trial-based free recall experiments, individual stimuli encountered during encoding are typically labeled as “remembered” or “forgotten” depending on whether the stimulus is recalled/recognized during a subsequent test. While this approach has advanced our understanding of human memory immensely, it does not translate well to naturalistic experiences. For one thing, the contents of our recall at any given moment might be reflected in many prior experiences/moments. Furthermore, the particular words used to describe the experience will inevitably vary across people and even across repeated recollections within an individual. Thus, there is not a “one-to-one” mapping between naturalistic experiences and their mnemonic counterparts. For example, remembering the patterns and colors of each person’s shirt in a crowd might be considered as excellent recall in a standard memory task setup. But if the rememberer failed to note that the people in the crowd were gathered for their surprise birthday party, then they would have missed the “point” of the experience.

Our topic modeling approach, whereby we consider the broad “theme” present in different moments of participants’ experiences and their memories for those experiences, affords us the ability to flexibly and accurately characterize memory for naturalistic experiences. This approach allows us to quantify which moments from the past and the current recounted experience match in terms of their thematic content and critically, our ability to perform this matching does not require participants to use any specific overlapping words. Our work characterizes recollection of an experience by comparing the overall “shape” of a dynamic stimulus and a memory. We assess the quality of memory for the video participants viewed by measuring the match between the shapes of the video’s trajectory and each participant’s recall trajectory. By contrast, the number of recalls could be captured by the “sampling frequency” along that trajectory – but the number of recalls alone cannot tell us whether participants successfully recollected the meaning of the story by capturing the salient points of the narrative that define its main shape. In addition to providing a way to capture the shape of an experience, this method affords the ability to quantify the particular contents of memory. Whereas traditional approaches abstract over the content (e.g., percent correct), Our approach allows one to quantify which aspects of an experience are memorable and which fail to stick. This aspect of our approach opens the door for a much richer characterization of memory that considers not just how much information was recalled, but the particular details of that information as well.

Prior work on neural responses during naturalistic experiences and recall has largely focused on identifying brain regions whose responses are reliably similar across individuals (Lerner et al., 2011; Simony et al., 2016; Chen et al., 2017; Baldassano et al., 2017; Zadbood et al., 2017). This allows one to identify which regions might be processing or representing the stimulus, or retrieving details of the experience during recall. Our approach is fundamentally different. We ask: which brain regions during video viewing match the video structure and how individual participants will recall the video later (in terms of the temporal correlations of their recall topic trajectory)? This latter approach highlights regions such as the medial prefrontal cortex (mPFC) and medial temporal lobes (MTL) that may respond in idiosyncratic ways across individuals, but that nonetheless play an important role in encoding experience into memory. In other work, the mPFC has been suggested to play a role in the representation of a “schema”, or a network of prior knowledge that is consistent with the current task (van Kesteren et al., 2012; Gilboa and Marlatte, 2017). One interpretation for mPFC’s involvement in our work is that mPFC represents participant-specific relationships with the content of the video, and its representation during scene viewing is related to how a participant later describes the scene. MTL activity patterns also matched participant’s recall, which is consistent with a large body of literature highlighting the role of the MTL in episodic memory encoding (Paller and Wagner, 2002; Davachi et al., 2003; Ranganath et al., 2004; Davachi, 2006).

More broadly, these findings have strong implications for how we assess memory in other naturalistic contexts, such as the classroom or in a doctor’s office. Whereas academic tests often measure students’ performance using metrics such as the proportion of correctly answered questions, our work suggests that this approach might “miss the forest for the trees”. We view “true learning” as understanding key concepts (i.e., understanding central themes in the learned content and how they relate) rather than regurgitating the greatest number of facts. In addition to educational contexts, our approach may provide unique metrics that can be used to assist in the diagnosis of memory disorders, and other psychiatric disorders that influence memory. For example, while the quantity of information recalled could be roughly matched between a healthy and patient population, and other aspects of the memory (such as the shape, serial order, precision or distinctiveness) might be different. Thus, this work serves as a foundation for more nuanced approaches to memory assessment that consider the trajectory and specific contents of memory for a naturalistic experience.

An important question for future work concerns the factors that drive an individual to sample their recall trajectory finely or coarsely. For example, given a short recall interval, would participants intuitively gravitate towards coarser samplings that still outline the basic shape of the video’s topic trajectory? Or if participants were told that their narrations would be played back to other participants (Zadbood et al., 2017), would that change the resolution or shape of their recalls? And over successive recounts of the same sequence of events or with more elapsed time between encoding and recall, how do the shapes of the trajectories change? For example, loss of detail would result in a “smoothing out” of the trajectories with each new retelling.

While we view this work as a major advance in characterizing and understanding human memory, as with any approach there are limitations. First, the approach relies on having a “good” model of the stimulus (e.g., one that describes the video in the same way as participants recall it), which is currently only achievable by a human hand-annotating each moment of the video. To increase the scalability of this approach, future work could explore automated methods for extracting meaning from videos (Haonan et al., 2016). Another potential limitation is that by its nature, the model extracts the “gist” of scenes from the video. This provides desirable flexibility

(e.g., participants can use different combinations of words to describe the scenes), but this comes at the expense of capturing specific details. Thus, a future direction of this work will be to increase sensitivity to such details while maintaining flexibility.

To conclude, we'll revisit the question of what it means to remember something. Our view is that "successful remembering" is about recovering the "trajectory" of an experience, rather than the ability to recognize/recall any of its particular isolated details. Decades of research suggest that episodic memories are not veridical and context-free snapshots of the past, and so treating (and modelling) them as such is overly simplistic at best (and counterproductive at worst). While it's undeniable that these models have been useful in advancing our understanding of human memory, they are severely limited in their ability to explain memory for real life experiences. Real life experiences are highly structured in time, and so to have a complete understanding of the human memory system, our experiments and models of memory must not ignore this fact. Our work provides a theoretical advance in our understanding of what it means to remember as well as a novel methodological tool to study it.

References

- Baldassano, C., Chen, J., Zadbood, A., Pillow, J. W., Hasson, U., and Norman, K. A. (2017). Discovering event structure in continuous narrative perception and memory. *Neuron*, 95(3):709–721.
- Blei, D. M., Ng, A. Y., and Jordan, M. I. (2003). Latent dirichlet allocation. *Journal of Machine Learning Research*, 3:993 – 1022.
- Brunec, I. K., Moscovitch, M. M., and Barense, M. D. (2018). Boundaries shape cognitive representations of spaces and events. *Trends in Cognitive Sciences*, 22(7):637–650.
- Capota, M., Turek, J., Chen, P.-H., Zhu, X., Manning, J. R., Sundaram, N., Keller, B., Wang, Y., and Shin, Y. S. (2017). Brain imaging analysis kit.
- Chen, J., Leong, Y. C., Norman, K. A., and Hasson, U. (2017). Shared experience, shared memory: a common structure for brain activity during naturalistic recall shared experience, shared memory: a common structure for brain activity during naturalistic recall. *Nature Neuroscience*, 20(1):115–125.
- Clewett, D. and Davachi, L. (2017). The ebb and flow of experience determines the temporal structure of memory. *Curr Opin Behav Sci*, 17:186–193.
- Davachi, L. (2006). Item, context and relational episodic encoding in humans. *Current Opinion in Neurobiology*, 16(6):693—700.
- Davachi, L., Mitchell, J. P., and Wagner, A. D. (2003). Multiple routes to memory: distinct medial temporal lobe processes build item and source memories. *Proceedings of the National Academy of Sciences, USA*, 100(4):2157 – 2162.
- DuBrow, S. and Davachi, L. (2013). The influence of contextual boundaries on memory for the sequential order of events. *Journal of Experimental Psychology: General*, page In press.

- Ezzyat, Y. and Davachi, L. (2011). What constitutes an episode in episodic memory? *Psychological Science*, 22(2):243–252.
- Gilboa, A. and Marlatt, H. (2017). Neurobiology of schemas and schema-mediated memory. *Trends Cogn Sci*, 21(8):618–631.
- Haonan, Y., Jiang, W., Zhiheng, H., Yi, Y., and Wei, X. (2016). Video paragraph captioning using hierarchical recurrent neural networks. In *Proceedings of the IEEE conference on computer vision and pattern recognition*, pages 4584–4593.
- Heusser, A. C., Ziman, K., Owen, L. L. W., and Manning, J. R. (2018). HyperTools: a Python toolbox for gaining geometric insights into high-dimensional data. *Journal of Machine Learning Research*, 18(152):1–6.
- Hogan, R. M. (1975). Interitem encoding and directed search in free recall. *Memory & Cognition*, 3:197–209.
- Howard, M. W. and Kahana, M. J. (1999). Contextual variability and serial position effects in free recall. *Journal of Experimental Psychology: Learning, Memory, and Cognition*, 25:923–941.
- Howard, M. W. and Kahana, M. J. (2002). A distributed representation of temporal context. *Journal of Mathematical Psychology*, 46:269–299.
- Howard, M. W., MacDonald, C. J., Tiganj, Z., Shankar, K. H., Du, Q., Hasselmo, M. E., and H., E. (2014). A unified mathematical framework for coding time, space, and sequences in the medial temporal lobe. *Journal of Neuroscience*, 34(13):4692–4707.
- Kahana, M. J. (1996). Associative retrieval processes in free recall. *Memory & Cognition*, 24:103–109.
- Koriat, A. and Goldsmith, M. (1994). Memory in naturalistic and laboratory contexts: distinguishing accuracy-oriented and quantity-oriented approaches to memory assessment. *Journal of Experimental Psychology: General*, 123(3):297–315.
- Laming, D. (1999). Testing the idea of distinct storage mechanisms in memory. *International Journal of Psychology*, 34:419–426.
- Lerner, Y., Honey, C. J., Silbert, L. J., and Hasson, U. (2011). Topographic mapping of a hierarchy of temporal receptive windows using a narrated story. *Journal of Neuroscience*, 31(8):2906–2915.
- Manning, J. R., Norman, K. A., and Kahana, M. J. (2015). The role of context in episodic memory. In Gazzaniga, M., editor, *The Cognitive Neurosciences, Fifth edition*, pages 557–566. MIT Press.
- McInnes, L. and Healy, J. (2018). Umap: Uniform manifold approximation and projection for dimension reduction. *arXiv*, 1802(03426).
- Murdock, B. B. (1962). The serial position effect of free recall. *Journal of Experimental Psychology*, 64:482–488.
- Paller, K. A. and Wagner, A. D. (2002). Observing the transformation of experience into memory. *Trends in Cognitive Sciences*, 6(2):93–102.

- Pedregosa, F., Varoquaux, G., Gramfort, A., Michel, V., Thirion, B., Grisel, O., Blondel, M., Prettenhofer, P., Weiss, R., Dubourg, V., Vanderplas, J., Passos, A., Cournapeau, D., Brucher, M., Perrot, M., and Duchesnay, E. (2011). Scikit-learn: Machine learning in Python. *Journal of Machine Learning Research*, 12:2825–2830.
- Polyn, S. M., Norman, K. A., and Kahana, M. J. (2009). A context maintenance and retrieval model of organizational processes in free recall. *Psychological Review*, 116(1):129–156.
- Rabiner, L. (1989). A tutorial on Hidden Markov Models and selected applications in speech recognition. *Proceedings of the IEEE*, 77(2):257–286.
- Radvansky, G. A. and Zacks, J. M. (2017). Event boundaries in memory and cognition. *Curr Opin Behav Sci*, 17:133–140.
- Ranganath, C., Cohen, M. X., Dam, C., and D’Esposito, M. (2004). Inferior temporal, prefrontal, and hippocampal contributions to visual working memory maintenance and associative memory retrieval. *Journal of Neuroscience*, 24(16):3917–3925.
- Ranganath, C. and Ritchey, M. (2012). Two cortical systems for memory-guided behavior. *Nature Reviews Neuroscience*, 13:713 – 726.
- Simony, E., Honey, C. J., Chen, J., and Hasson, U. (2016). Uncovering stimulus-locked network dynamics during narrative comprehension. *Nature Communications*.
- van Kesteren, M. T. R., Ruiter, D. J., Fernández, G., and Henson, R. N. (2012). How schema and novelty augment memory formation. *Trends Neurosci*, 35(4):211–9.
- Yonelinas, A. P. (2002). The nature of recollection and familiarity: A review of 30 years of research. *Journal of Memory and Language*, 46:441–517.
- Zacks, J. M., Speer, N. K., Swallow, K. M., Braver, T. S., and Reynolds, J. R. (2007). Event perception: a mind-brain perspective. *Psychological Bulletin*, 133:273–293.
- Zadbood, A., Chen, J., Leong, Y. C., Norman, K. A., and Hasson, U. (2017). How we transmit memories to other brains: Constructing shared neural representations via communication. *Cereb Cortex*, 27(10):4988–5000.
- Zwaan, R. A. and Radvansky, G. A. (1998). Situation models in language comprehension and memory. *Psychological Bulletin*, 123(2):162 – 185.

Methods

Participants and Experimental Design

Participants ($n = 17$) viewed the first 50 minutes of “A Study in Pink”, an episode of the BBC series, *Sherlock*. Immediately upon completion of the video, participants were instructed to (verbally) recount the events in the *Sherlock* episode in their original order and in as much detail as possible. During the entire experiment, participants were in an fMRI scanner. For comprehensive details of the experimental procedures, please refer to Chen et al. (2017).

Fitting the topic model to the video text and recall transcripts

A topic model was used to estimate the most likely mixture of topics for a given sample of text. First, the video was manually segmented into 1000 scenes, and a collection of descriptive features was manually transcribed. For each scene, we considered the following features: narrative details (a sentence or two describing what happened in that scene), whether the scene was indoor or outdoor, name of all the characters in the scene, name of the character in focus, name of the character speaking, location, camera angle, music presence, and text on the screen. We concatenated the text for all of these features within each segment, creating a “bag of words” describing each scene. We then transformed the text descriptions into overlapping windows of 50 scene segments. For example, the first text sample comprised the text from the first 50 segments, the 2nd comprised the text from $n+1:n+51$, and so on. We trained our model using these overlapping text samples with scikit-learn’s (version 0.19.1) ‘CountVectorizer’ and ‘LatentDirichletAllocation’ classes (Pedregosa et al., 2011) implemented using our high-dimensional visualization/analysis software, Hypertools (Heusser et al., 2018). First, the text was transformed into a vector of word counts (after removing English stopwords). This gave a word count vector for each scene in the video. Then, the word count vectors were used to fit a topic model (topics=100, method='batch'). We transformed the text descriptions using the model resulting in a scenes (1000) by topics (100) matrix. The scene descriptions often spanned multiple timepoints (i.e., TRs). To account for this, we expanded the video model by copying the rows of the model for as many timepoints that the scene description spanned. After this expansion, the shape of the model was the length of the duration of the video (1976 TRs).

To create the recall models, for each participant we tokenized the recall transcript into a list of sentences and then mapped the list to overlapping windows of 10 sentences. We transformed the list of overlapping recall sentences using the model that was trained on the video text (as described in the paragraph above). The result of this was a sentences (range: 68-294) by topics (100) matrix for each participant that represented the most likely mixture of topics for a given chunk of sentences.

Choosing topic model parameters

There were 3 critical parameters related to fitting the topic model: 1) the number of topics, 2) the window size of text descriptions of the video used to fit the model, and 3) the window size of recall sentences used to transform the recall data. To chose these parameter values, we performed a grid search where the range of possible parameter values was 1, 5, 10, 25, 50, 100, 200, and 500. Our optimization objective was defined as the correlation between the hand annotated memory performance and the root mean squared distance between the video model and the recall model before any further processing (e.g., hidden Markov modelling, averaging within event, etc). While many of the parameter combination elicited moderately high correlations, the optimal choice was 100 topics, 50 video segments and 10 recall sentences.

Extracting events using a hidden Markov model

The topic model timepoint-by-timepoint correlation matrices all exhibited a block-diagonal structure (with small off-diagonal values), suggesting that the models were comprised of a number of sequential ‘states’ (or events, see Supp. Fig. 1). To capture this structure, we fit the video and each recall model using a hidden Markov model (HMM). Given a number of states or events (k), the HMM recovers a set of labels that segments consecutive timepoints into k events (Rabiner, 1989;

Baldassano et al., 2017). To implement this analysis, we used the Brainiak toolbox (Baldassano et al., 2017; Capota et al., 2017).

Our metric for choosing the “best fitting” HMM was to choose the model with the k value that maximized the ratio of the average ‘within-event’ correlation values (i.e., the correlation values for blocks of consecutive timepoints the model identified as one event) and the average ‘across-event’ correlation (i.e., the rest of the correlation values). Additionally, we included a penalty parameter that was proportional to the smoothing of the model that preferred models with smaller k values. We chose k values separately for the video model and for each recall model. Then, using the best k values, We fit a separate HMM for the video and each recall model. Finally, we averaged over timepoints identified to be in the same event resulting in a events by topics matrix for the video model and each of the recall models.

Matching recall events to video events

To estimate which video event each recall event referred to, we correlated the video events model and each recall events model. This resulted in a video events (34) by recall events (8-27) correlation matrix (for each participant) which contains the similarity between each video event and each recall event (see Supp. Fig. ??). To find the most likely video event that a given recall event referred to, we computed the argmax over the columns of this matrix. The result was a list of video event indices for each participant. These indices are analogous to the values found in a “recall matrix” from a free recall list learning experiment, but represent the recall of particular events (instead of words, for example).

Visualizing the video and recall event models

To visualize the temporal structure of the video event model (34 events by 100 topics) and the recall event models (8-27 events by 100 topics), we used a technique called UMAP (McInnes and Healy, 2018) to reduce the “topic-space” from 100 dimensions down to 2 dimensions. UMAP is a nonlinear dimensionality reduction technique which models the manifold of the data with a fuzzy topological structure, and then searches for a (2D) projection of the data that has the closest equivalent fuzzy topological structure. We concatenated (vertically stacked) all event models (video, average recall, and individual recall), and then fit and transformed all of the models at once. This assured that the models were projected into the same space.

Vector field analysis

To quantify the flow of recall from event to event, we performed a vector field analysis. We tiled the 2D topic space ($x, y: -6$ to 6 by .25) with an evenly spaced grid. For each grid point, we drew a circle around the point (radius=.5). Then, we tested whether any line segments (formed by event recall transitions) passed through this area of the topic space. For example, say that a participant transitioned from recalling event 2 to event 3. These 2 recall events correspond to 2 points in topic space, and connecting them forms a line segment. We collected all line segments that passed through a given section of topic space (collapsing across participants). To plot the average direction of the line segments (i.e., the arrows for each grid point in Fig. 3B), we converted each of them to unit vectors and then averaged. For grid points where the direction was consistent (across all participants contributing to that point), the length of the arrow approaches 1, whereas if the direction was random the length of the arrow approaches 0. Lastly, we converted each unit

vector to an angle (in radians) by taking the inverse tangent of the x, y components of the vector. To test whether the distribution of angles was significantly non-uniform (i.e., displayed a preferred direction across participants), we performed a Rayleigh test on the angles ($p < .001$, FDR-corrected at $p < .05$ using Benjamini-Hochberg procedure). Arrows where the Rayleigh test was significant are displayed in color (the darker the blue the more significant) while non-significant tests are displayed in gray with lower opacity.

fMRI analyses

Participants viewed and recalled the video stimulus inside an fMRI scanner. The video was split into two parts of approximately equal length (946 and 1030 TRs, $TR = 1.5\text{seconds}$). All data were preprocessed and transformed to 3mm MNI space as described in (Chen et al., 2017). Data were z-scored across time at every voxel. 6mm smoothing was applied. Files are cropped so that all video-viewing data are aligned across participants, and all recall data are aligned to the scene timestamps below. The cropping includes a constant 3-TR (4.5 sec) shift to correct for hemodynamic lag.

Searchlight analysis

Our multivariate analyses were designed to capture brain regions whose timepoint-by-timepoint correlational structure mirrors the correlational structure of the video model as well as participant-specific recall topic models during video viewing. We conducted a searchlight analysis (5x5x5 voxel cube) where for each cube, we correlated the model timepoint-by-timepoint correlation matrix with the neural correlation matrix. To aggregate across participants, we Fisher's z-transformed the correlations and then averaged. To assess significance, we recomputed this group analysis 100 times, but randomly phase shifted the model by the same amount for each participant but different amounts for each permutation to build a null distribution of correlation values. Finally, we thresholded the group averaged correlation maps where the 'real' correlation value for a given voxel exceeded the 95th percentile of the null distribution. To correct for non-linearities between the viewing time and recall time, for each participant we used dynamic time warping to temporally align the matrices. The algorithm recovers a path of coordinates that would bring the video and recall model in maximal temporal alignment. We used this path to warp the fMRI data and the recall model into temporal alignment (separately for each participant).

Topic vector word clouds

We created word clouds to visualize the themes contained in the recall events. One component of the topic model comprises a words (2117) by topics (100) matrix (R), where the rows represent the weight of a given word in each topic. To find words that were maximally associated with a particular event vector, we computed the dot product between R and v, which gave a 1 by # of words vector where the values represent the "activation" of each of in the event. Activation is defined as the weight of a particular word in a particular event. Then, we created word clouds by extracting the top n words and plotting them where the size of the word is proportional to its activation in the event.

In the first analysis (Fig. 5A,B), we quantified the most and least remembered topics/words throughout the entire video by computing a weighted average over all recall events, where the

weights were proportional to memory for each recall event. To measure memory for each event, for each participant we computed the correlation between the video event vector and the closest recall event vector. We then averaged these correlation values across participants. We then computed a weighted average of all video events using the correlation values as weights. Next, we computed the dot product between this weighted-average video event vector and the R matrix (described in the paragraph above) to get activations for each word. Finally, we plotted the top 200 words where the size of the word is proportional to its activation. To get the least remembered topics/words, we performed the same analysis but inverted memory weights.

In the second analysis (Fig. 5C), we created wordles for the top/bottom 3 remembered video events indexed by the average correlation values (Fig. 5A). To get the “activations” for words associated with the video events, we computed the dot product between the video event vector and the R matrix. The same procedure was used to get word activations for the recall events. We then plotted the top 200 words for the top/bottom 3 recalled events.

Supplemental Materials: How is experience transformed into memory?

Naturalistic extensions of classic list-learning analyses

Just like in a traditional free recall list-learning experiment where participants view a list of words and then verbally recall them, our video-recall matching analysis approach affords us the ability to analyze memory in the same way. The recalled events can be treated as “items” analogous to words recalled in a list-learning study. Here, we sought to characterize memory performance/dynamics by extending classic analyses originally designed for list-learning experiments to more naturalistic settings.

First, we asked whether the estimated number of recall events (k) by participant was related to hand-annotated accuracy as published in Chen et al. (2017). We found a strong positive correlation where participants with a greater number of recall events also had better overall memory performance (Pearson’s $r(16) = .67, p = .003$). Then, we considered how participants initiated the recall sequence (known in the literature as the ‘probability of first recall’ or ‘PFR’). We found that participants tended to initiate their recall sequences with the first few events (Supp. Fig. 4A), which is qualitatively very similar to previously published list learning experiments (Howard and Kahana, 1999). Next, we considered another well-studied memory measure in the list-learning literature, the lag conditional response probability curve (or lag-CRP) (Kahana, 1996). The result suggests a strong bias to transition sequentially events in the forward direction (Supp. Fig. 4B). Finally, we assessed memory performance for each event in the video as a function of its serial position during encoding (Supp. Fig. 4C). We did not observe the classic “primacy” and “recency” pattern which is prevalent in the literature (Murdock, 1962). We also considered two additional across-participant measures of recall that characterize memory organization: temporal clustering and semantic clustering. We found that participants who clustered in time also recalled a greater number of events (Pearson’s $r(16) = .62, p = .007$). Next, we assessed semantic clustering. We found that the semantic clustering score was related to memory performance across participants (Pearson’s $r(16) = .55, p = .02$). Thus, participants who organized their recalls with respect to the semantic information contained in the scene had better memory performance.

Additional measures of naturalistic memory

To quantify the similarity between the video model and individual recall models, we considered a number of novel metrics. First, we tested whether each participant’s recall model matched the video model in a general sense. To do this, for each participant we filtered the video model to only include the events that the participant remembered and computed the root mean squared difference (RMSD) between the video model and the recall model. As an example, if the participant remembered all the events in order (with perfect precision), the expected distance value would be 0. However, if they remembered a subset of events, events out of order, or with low precision, the expected distance would be greater than 0. To assess significance, we performed a permutation test where we circularly shifted the recall model (10000 times) and recomputed the RMSD. The recall model significantly matched the video model for nine of the participants ($p < .05$, participants: 3-4, 8-13, 17 and the p-value for the rest of the participants was less than .25). Furthermore, the RMSD values were significantly correlated to hand annotated memory performance across participants

(Pearson's $r(16) = -.57, p = .016$). Thus, a closer match between the video and recall event models was related to better recall performance.

Next, we tested whether participants who recalled more events were also more precise in their recollections. For each participant, we computed the correlation between each recall event and its matching video event (only for the events which they recalled). This resulted in a single number for each recalled event indexing how similar the recall event was to its matching video event (i.e the "precision" of the recall). We then averaged the correlations within participant. In line with our prediction, there was a strong correlation between hand annotated memory performance and precision suggesting that participants who remembered more events also remembered them more veridically (Pearson's $r(16) = .74, p = .0006$).

Then, we considered the distinctiveness of each recall event. That is, how uniquely a recall event matched a given video event compared to all other video events. We hypothesized that participants with high memory performance might describe each event in a more distinctive way (relative to those with lower memory performance who might describe events in a more general way). To this end, we computed a 'distinctiveness' score for each participant (i.e., $1 - \text{the correlation between a recall event and all non-matching video events}$). Then, we averaged this measure over recall events within participant. We found that participants with higher hand annotated memory performance also had higher distinctiveness scores (Pearson's $r(16) = .8, p = .0001$).

Lastly, we tested whether participants with better memory performance were also more likely to remember the events in order. For each participant, we computed the Spearman rank correlation between the order of events that the participant recalled and the actual order of events (filtering events that were actually recalled). We found that participants who recalled more events also recalled more of them in order (Pearson's $r(16) = .5, p = .04$). In summary, we found that better memory performance was associated with more precise, distinctive and ordered recalls.

Supplemental Methods

Quantifying the importance of features

To determine the contribution of each feature to the structure of the video model, we examined the similarity between the temporal structure of models trained in the absence of a single feature and that of our original (i.e., full) model (Supp. Fig. 3A). First, we iteratively removed one transcribed feature from the scene descriptions and constructed a timepoints (1976) by topics (100) matrix using a topic model fit to the remaining features. We then represented the original model as well as the new model's temporal structure as a timepoints-by-timepoints correlation matrix. Finally, we vectorized these correlation matrices and correlated them to each other resulting in a single number (for each feature removed from the model) representing the similarity of the "feature-removed" models to the full model.

In order to ascertain which features were important in relating the recall models to the video model, we similarly compared to the temporal structures of video and recall models deprived of a single feature at a time (Supp. Fig. 3B). For each feature removed, we transformed each participant's recall transcript using a model trained on the feature-deprived video text windows (of 50 scene segments), and resampled the recall timeseries to match the shape of the video model (1976 timepoints). We then represented the temporal structures of each participant's recall model as timepoints-by-timepoints correlation matrices and computed the average correlation with the temporal structure of the video model (across participants).

List-learning analyses

Overall Accuracy. To get an overall measure of the quantity of information recalled, we computed the proportion of successfully recalled events by counting the number of unique recall events identified by the HMM model and dividing by the total number of video events. We performed this analysis for each participant separately.

Probability of first recall (PFR). The (PFR) analysis represents the probability that an item will be recalled first as a function of its serial position during encoding. We initialized a # of participants (17) by # of video events (34) matrix. Then for each participant, we found the index of the video event that was recalled first and filled in that index in the matrix with a 1. Finally, we averaged over the rows of the matrix, resulting in a 1 by 34 array representing the proportion of participant that recalled an event as a function of serial position during encoding.

Lag conditional probability curve (lag-CRP). The lag-CRP represents the probability that the next item recalled will be of lag i from the just recalled item. For each recall transition, we computed the lag between the current recall event and the next recall event, normalizing by the total number of possible transitions. This resulted in a # of participants (17) by lags (-33:+33) matrix. We averaged over the rows of this matrix to get a group-averaged lag-CRP.

Serial position curve (SPC). The SPC represents the proportion of participants that remember an item as a function of its serial position during encoding. We initialized a # of participants (17) by # of video events (34) matrix. Then, for each recall event (and each participant), we found the index of the video event that was recalled and filled it in with a 1. This resulted in a matrix where 1s indicate the successful recall of an event in serial position n and zeros indicate the lack of recall for that event. Lastly, we averaged over the rows of the matrix to get a 1 by 34 array representing the proportion of participants that recalled an event as a function of its serial position.

Temporal clustering. Temporal clustering measures the extent to which participants group their recall responses according to encoding position (Polyn et al., 2009). For instance, if the participant recalled each item in the presentation order, this would result in a score of 1. If the participant recalled randomly with respect to presentation order, this would result in a score of .5. For each event transition (and separately for each participant), we computed the rank similarity (euclidean distance) between the presentation position of the current and next recall events. The scores were then averaged within participant to get a single number representing the extent of temporal clustering exhibited by a given participant.

Semantic clustering. Similar to temporal clustering, semantic clustering measures the extent to which participants group their recall responses according to semantic similarity (Polyn et al., 2009). Here, we are using the topic vectors for each event as a proxy for its semantic content. Thus, similarity between the semantic content for two events can be computed by correlating their respective topic vectors. For instance, if each consecutive recall was the next most similar event (in terms of its s), this would result in a score of 1. If the participant recalled randomly with respect to semantic similarity, this would result in a score of .5. For each event transition (and separately for each participant), we computed the rank similarity (correlation distance) between the current recall event and the next recall event. The scores were then averaged within participant to get a single number representing the extent of semantic clustering exhibited by a given participant.

Additional measures of naturalistic memory

Precision. This measure gives us an indication of the specific match between a video event and recall event, where values approaching 1 are highly precise and lower values are imprecise. We

defined “precision” as the correlation between a recall event and its matching (i.e., argmax) video event.

Distinctiveness. Distinctiveness quantifies how similar a recall event is to all non-matching video events. It provides a metric of how uniquely a particular recall event describes a particular video event. To compute it, a given recall event is correlated to all video events, the argmax is removed and the rest of the values are averaged. The resulting value is subtracted from 1 such that larger values indicate a more distinctive recall event.

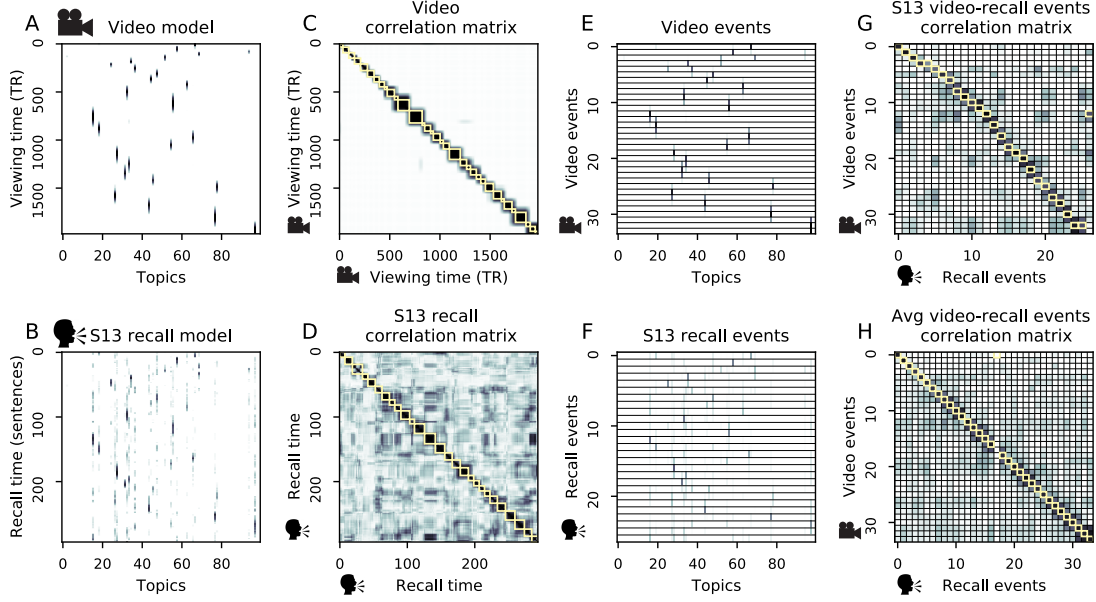


Figure 2: Modelling naturalistic stimuli and recall. A depiction of our analysis pipeline. For all plots, darker colors indicate greater values and the range of each plot is 0-1. **A.** A timepoints (1976) by topics (100) matrix representing the video stimulus. Each row represents the most likely mixture of topics for a given timepoint (i.e., topic weights). Each column represents a different topic. **B.** A sentences (294) by topics (100) matrix representing participant #13's recall. **C.** A viewing-time (1976) by viewing-time (1976) correlation matrix representing the correlation of each moment of the video model with every other moment of the video model. The yellow boxes represent 'events' recovered by a hidden Markov model. **D.** A recall-time (294 sentences) by recall-time (294) correlation matrix for participant #13. **E.** An events (34) by topics (100) matrix where each row represents the average topic vector for each event in the video model. **F.** An events (27) by topics (100) matrix where each row represents the average topic vector for each event in participant #13's recall model. **G.** A recall events (27) by video events (34) correlation matrix for participant #13. The cells with a yellow border identify the video event with the highest correlation to a given recall event. **H.** A group averaged recall events (34) by video events (34) correlation matrix. The cells with yellow borders are the video event with the highest correlation to a given average recall event.

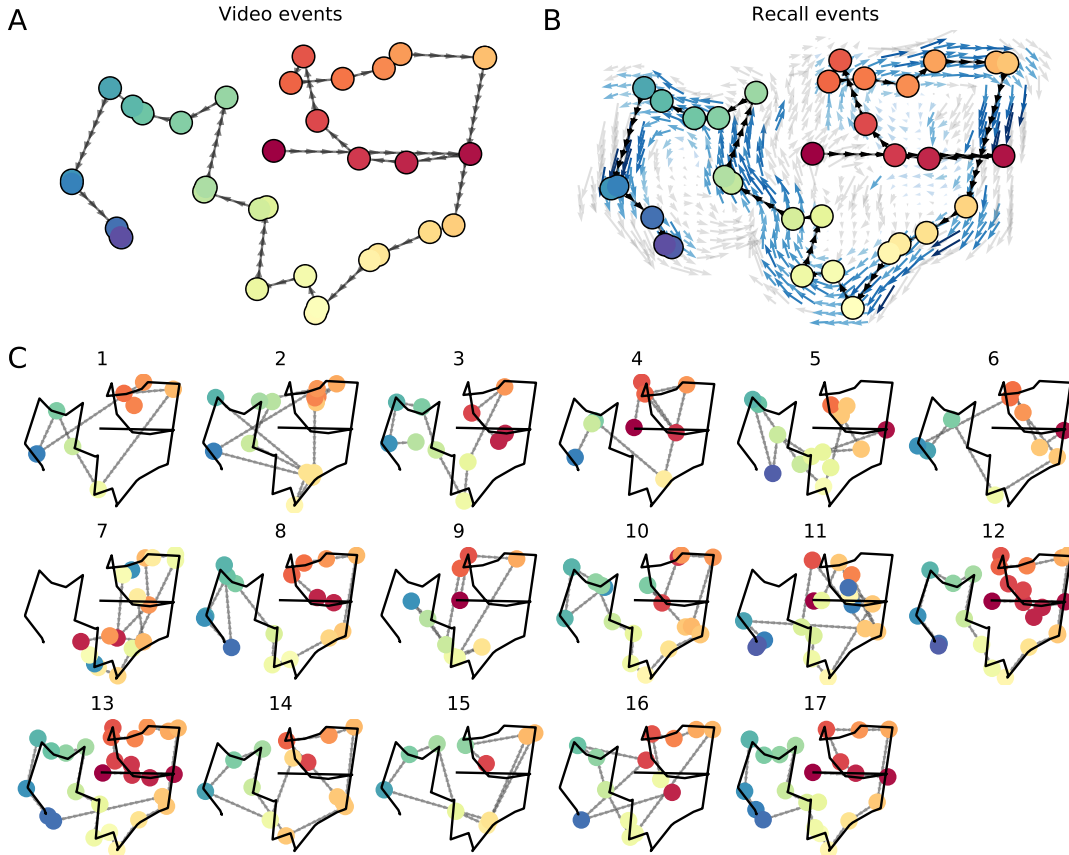


Figure 3: Video and recall trajectory plots. **A.** 2-dimensional embedding of the video events model (reduced with UMAP algorithm). The arrows indicate the forward direction of the video events. **B.** 2-dimensional embedding of the average recall events model. The colors refer to the most similar video events. The directional lines connecting the points represent the true video event order. The arrows represent the group-average direction of all recall event transitions (i.e., a line segment connecting two consecutive recall event vectors) that intersected a circle (radius=.5) centered on the origin of the arrow. **C.** Individual trajectory plots for each participant overlaid with the video model (black). The direction of the recall sequence is indicated by the direction of arrows connecting each recall event. The colors refer to the most likely video event.

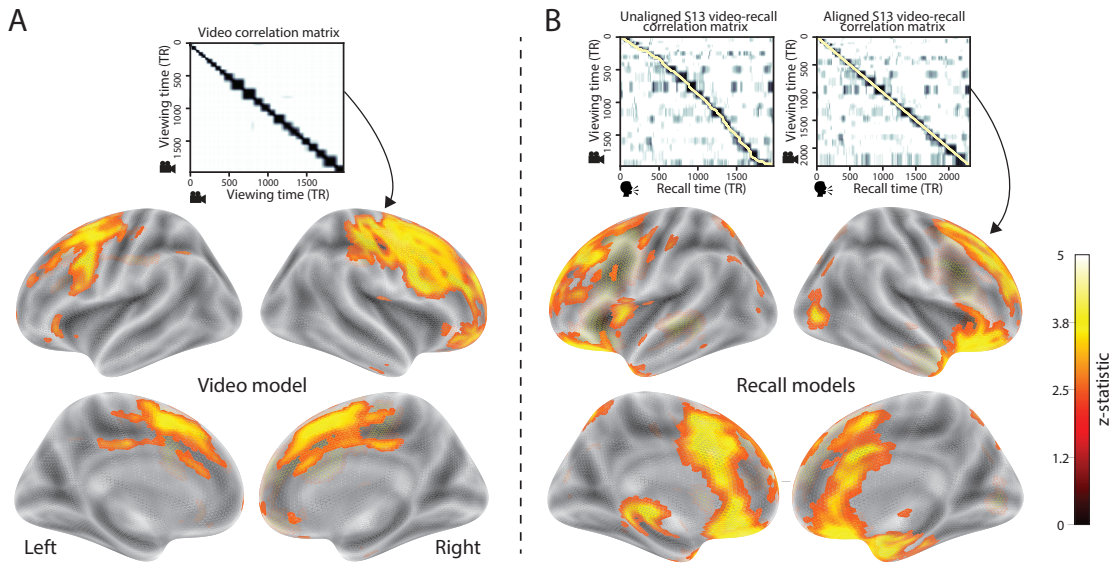


Figure 4: Video and recall model correlational structure searchlight analysis. **A.** The correlation matrix representing the temporal structure of the video model. Below it is a surface plot of brain regions whose activity patterns mirrored the correlational structure of video model during viewing. **B.** The left matrix is S13's video-recall correlation matrix before warping. The yellow stars represent the path recovered by dynamic time warping. The right matrix is the result after warping. The same warping path was applied to the fMRI timeseries (separately for each participant). A surface plot of brain regions whose activity patterns mirrored the participant-specific recall correlation matrix. Significance threshold ($p < .05$) for both video and recall analyses derived from a permutation procedure by phase shifting the video model and recomputing the z-scores.

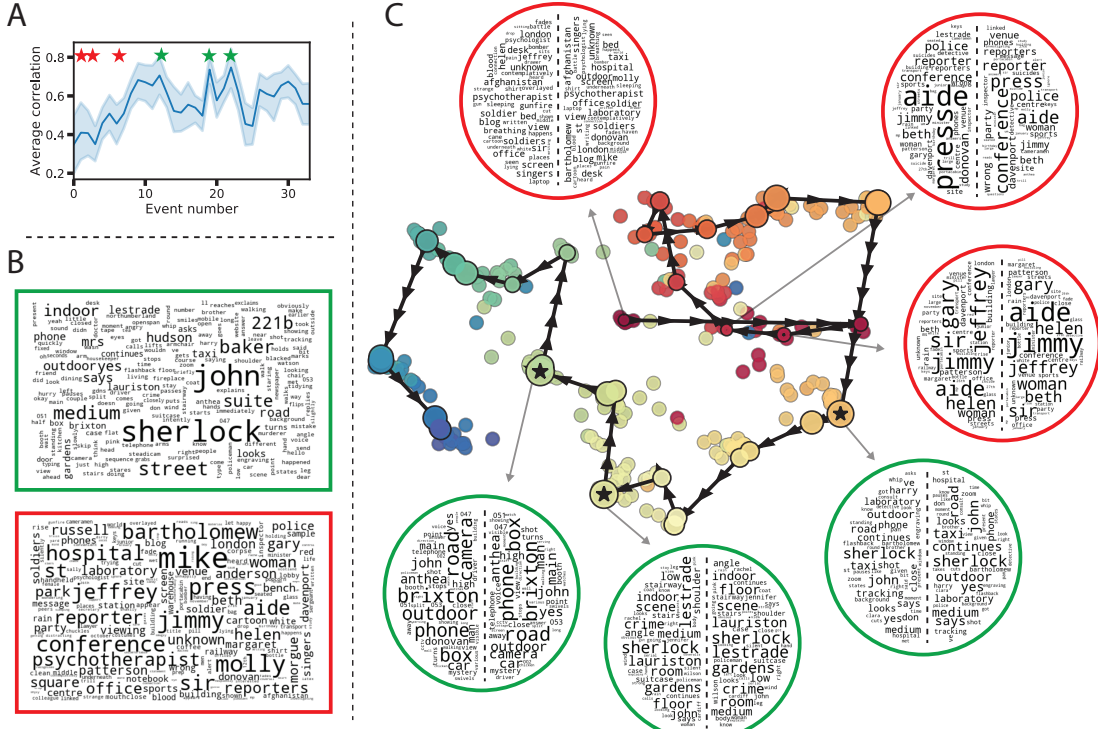
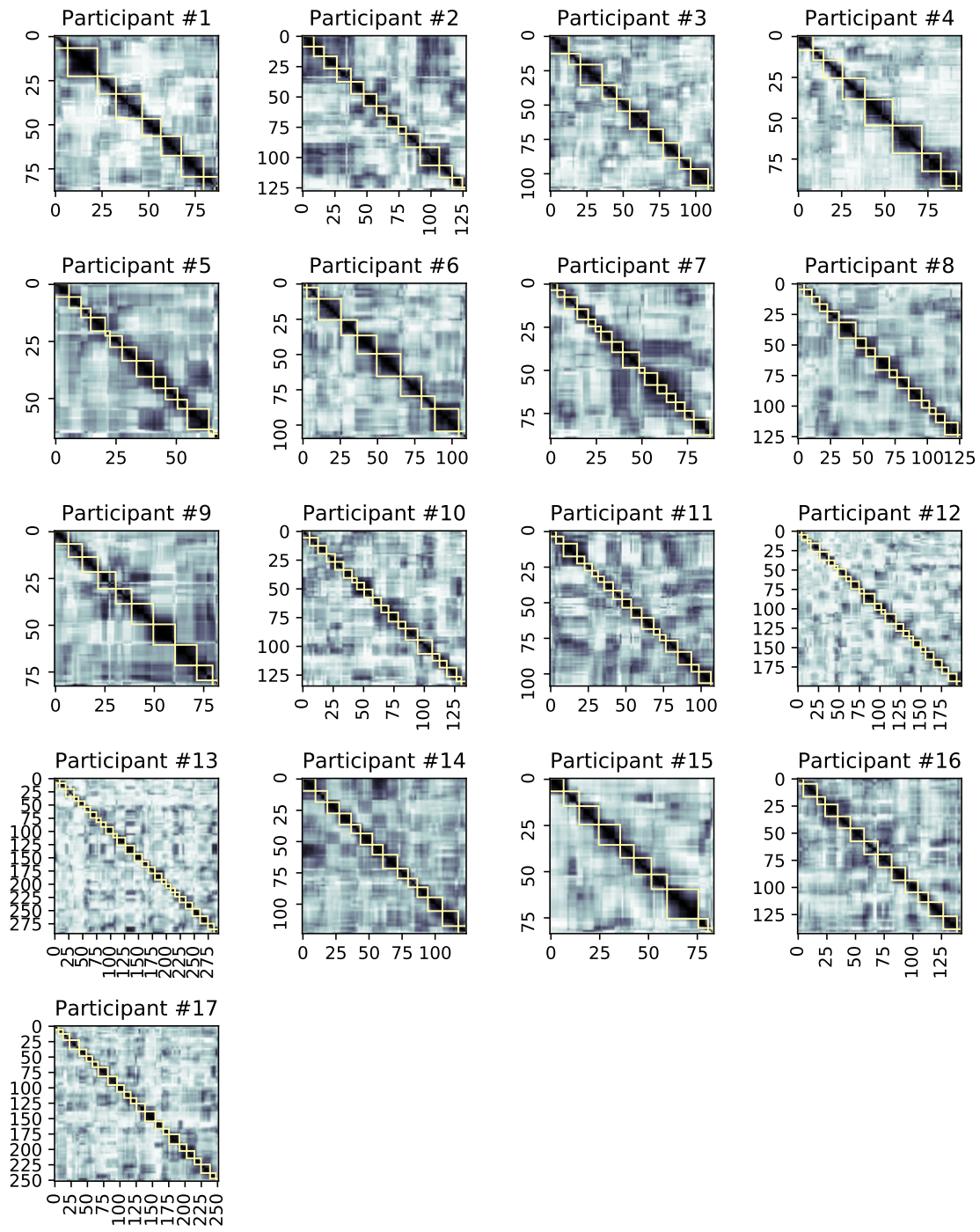
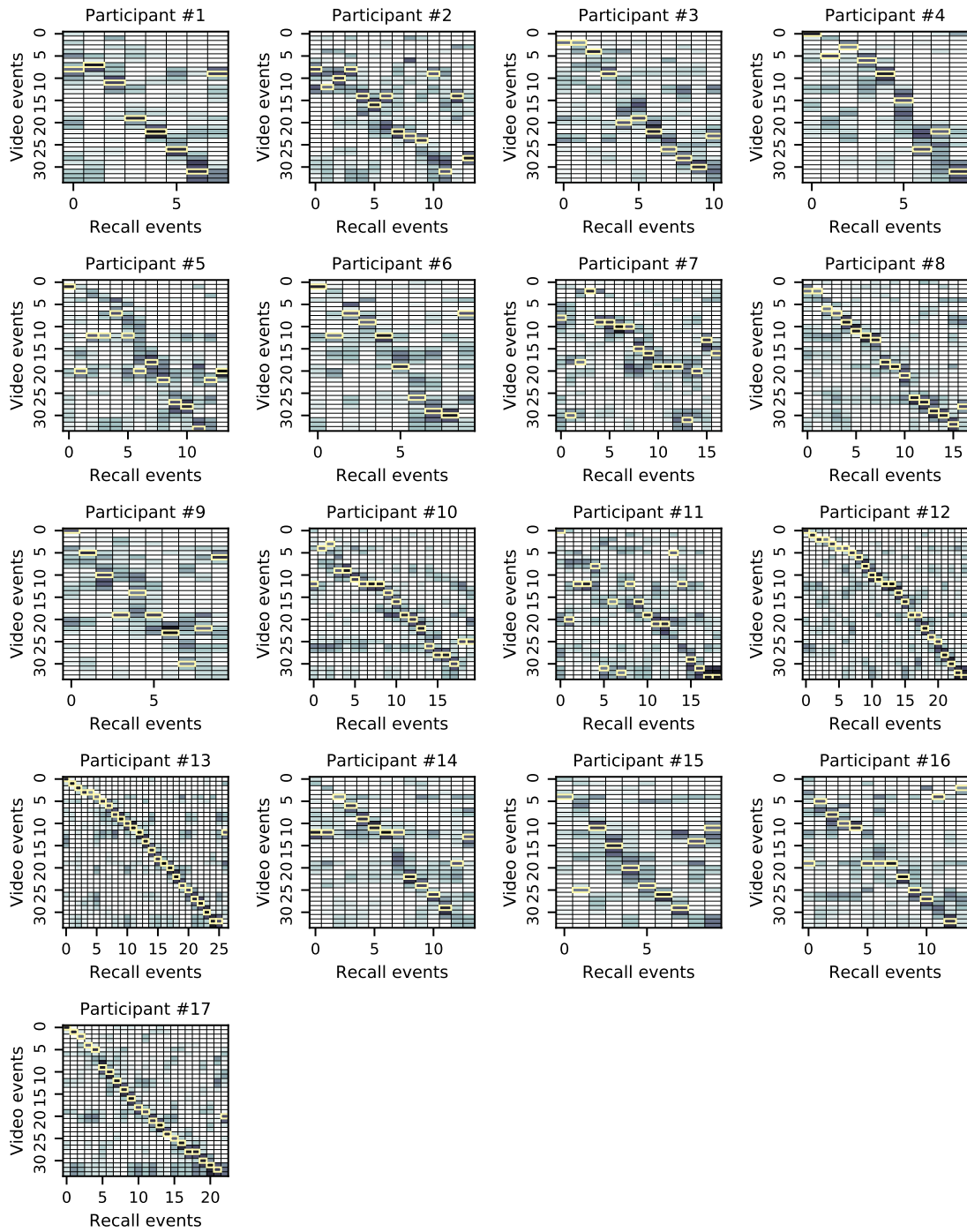


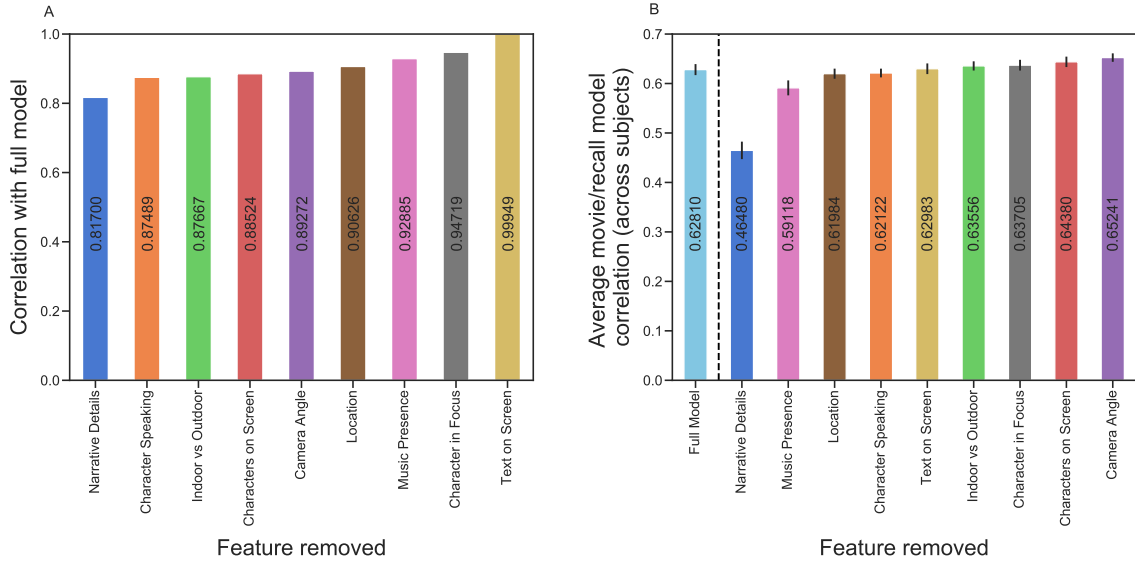
Figure 5: Analysis of topics by event memorability. **A.** Group-averaged correlation between each video event and closest recall event. Error bars represent 95% confidence intervals. Stars indicate top (green) and bottom (red) 3 remembered events across participants **B.** Wordles (top 200 words) representing a weighted average of video event topic vectors weighted by event memorability (e.g., the correlation values in A). The top wordle (green) contains words from the most remembered events and the bottom (red) contains words from least memorable events. The word sizes are proportional to the word's "activation". **C.** Trajectory represents the video event model embedded in a 2D space using UMAP. The large colored dots are video events. The small colored dots are individual recall events across all participants, where the colors correspond to the closest video event. The circular wordles represent the top 3 most (green circles) and least (red) memorable video events. The left side of the wordle circles contain words associated with the video event vector and the right side contains words associated with the average recall event vector.



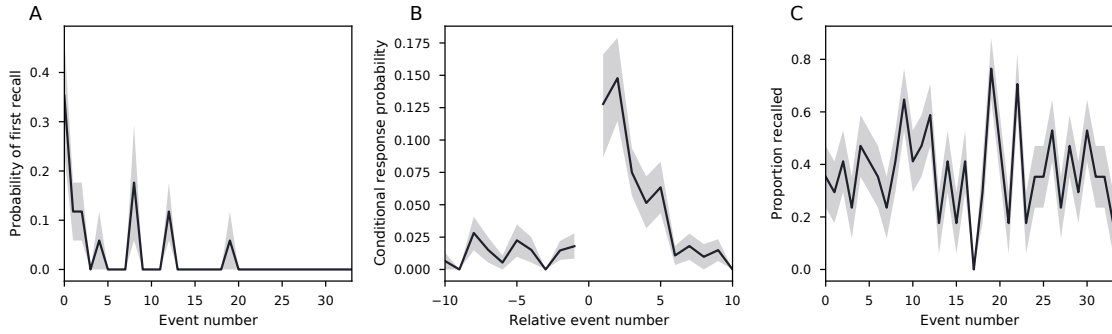
Supplementary Figure 1: Recall model correlation matrices and event segmentation fits. Each participant's timepoint-by-timepoint recall correlation matrix. The yellow boxes represent “events” identified by a hidden Markov model.



Supplementary Figure 2: Video-recall event model correlation matrices. Each participant's video event by recall event correlation matrix. The yellow boxes represent the maximum correlation in each column.



Supplementary Figure 3: Impact of individual features on topic modeling analysis. **A.** Contribution of each feature to model structure. Bars represent the correlation of a video model trained in the absence of a given feature to the model trained on all features. **B.** Contribution of each feature to video model/recall model relationship. The leftmost bar represents the across-participants mean correlation between the video model and recall models trained on all features. Subsequent bars represent the same relationship between video and recall models trained in the absence of a given feature. Error bars are the standard error of the mean across participants.



Supplementary Figure 4: Naturalistic extensions of classic list-learning memory analyses. **A).** The probability of first recall as a function of the serial position of the event during encoding. **B).** A lag-conditional response probability curve. Given recall of event i , the probability that the next recalled item will be from serial position $i + \text{lag}$. **C).** Proportion of events recalled as a function of serial position. All error bars are the standard error of the mean derived from a bootstrap resampling procedure.